Tissue-restricted control of established central nervous system autoimmunity by TNF receptor 2–expressing Treg cells

Emilie Ronin[a,1], Charlotte Pouchy[a,1], Maryam Khosravi[a], Morgane Hilaire[a], Sylvie Grégoire[a], Armanda Casrouge[a], Sahar Kassem[a], David Sleurs[a], Gaëlle H. Martin[a], Noémie Chanson[a], Yannis Lombardi[a], Guilhem Lalle[b], Harald Wajant[c], Cédric Auffray[d], Bruno Lucas[d], Gilles Marodon[a], Yenkel Grinberg-Bleyer[b,2,3], and Benoît L. Salomon[a,2,3]

[a]Sorbonne Université, INSERM, CNRS, Centre d'Immunologie et des Maladies Infectieuses (CIMI)–Paris, F-75013 Paris, France; [b]Centre de Recherche en Cancérologie de Lyon, Labex DEVweCAN, INSERM, CNRS, Université Claude Bernard Lyon 1, Centre Léon Bérard, 69008 Lyon, France; [c]Division of Molecular Internal Medicine, Department of Internal Medicine II, University Hospital Würzburg, 97070 Würzburg, Germany; and [d]Institut Cochin, CNRS, INSERM, Paris Université, F-75014 Paris, France

Edited by Shimon Sakaguchi, Osaka University, Osaka, Japan, and approved February 17, 2021 (received for review July 4, 2020)

CD4$^+$Foxp3$^+$ regulatory T (Treg) cells are central modulators of autoimmune diseases. However, the timing and location of Treg cell–mediated suppression of tissue-specific autoimmunity remain undefined. Here, we addressed these questions by investigating the role of tumor necrosis factor (TNF) receptor 2 (TNFR2) signaling in Treg cells during experimental autoimmune encephalomyelitis (EAE), a model of multiple sclerosis. We found that TNFR2-expressing Treg cells were critical to suppress EAE at peak disease in the central nervous system but had no impact on T cell priming in lymphoid tissues at disease onset. Mechanistically, TNFR2 signaling maintained functional Treg cells with sustained expression of CTLA-4 and Blimp-1, allowing active suppression of pathogenic T cells in the inflamed central nervous system. This late effect of Treg cells was further confirmed by treating mice with TNF and TNFR2 agonists and antagonists. Our findings show that endogenous Treg cells specifically suppress an autoimmune disease by acting in the target tissue during overt inflammation. Moreover, they bring a mechanistic insight to some of the adverse effects of anti-TNF therapy in patients.

Treg cells | autoimmune diseases | TNF

CD4$^+$Foxp3$^+$ regulatory T (Treg) cells play a pivotal role in the control of immune responses. In particular, the effector Treg cell subset, controlled in part by the master transcription factor Blimp-1 (1–3), exerts a critical role in the protection against autoimmune diseases by inhibiting autoreactive cells. Perturbations in Treg cell numbers or function trigger or exacerbate autoimmune diseases in mice and humans, such as type 1 diabetes, rheumatoid arthritis, or experimental autoimmune encephalomyelitis (EAE), a mouse model of multiple sclerosis (MS) (4, 5). In line with this latter observation, Treg cell depletion increased EAE symptoms (6), while transfer of polyclonal or myelin-reactive Treg cells limited the disease (7, 8). However, it is still unknown whether Treg cells suppress the priming of pathogenic conventional T (Tconv) cells in the draining lymph nodes (dLNs) at disease onset, and/or inhibit their function directly in the central nervous system (CNS) in the phase of ongoing inflammation.

Our group and others have reported that tumor necrosis factor (TNF) increased the proliferation of Treg cells via TNF receptor 2 (TNFR2) while maintaining or enhancing their suppressive function in vitro and in different immunopathologies (9–13). This intriguing immunoregulatory facet of TNF is clearly exemplified in EAE. Mice deficient for TNFR2 exhibited aggravated symptoms of EAE, which were associated with lower Treg cell proportions in the CNS (14). In the same line, mice genetically engineered to express the human version of TNF, and in which TNFR2 was ablated in Treg cells, developed severe EAE symptoms (15). These studies suggested that the TNF/TNFR2 axis is central in Treg cell–mediated suppression of autoimmunity. However, the location and timing of this Treg cell–mediated suppression are currently unknown. Here, we addressed these questions by using constitutive and inducible ablation of TNFR2 in mature Treg cells. We showed that TNFR2-expressing Treg cells suppressed EAE locally in the inflamed CNS on established disease, without affecting pathogenic T cell priming in the dLN.

Results

TNFR2 Expression by Hematopoietic Cells Is Required to Limit EAE Severity and Promotes Treg Cell–Intrinsic Expansion in the CNS. Since TNFR2 is up-regulated in Treg cells upon activation (9), we analyzed its expression after EAE induction. The receptor was highly and preferentially expressed in Treg cells at all time points in dLN and from day 10 in the inflamed CNS (*SI Appendix*, Fig. S1). To study the role of the TNF/TNFR2 axis in Treg cells during EAE, we first performed experiments with mice carrying germline deletion of TNFR2 (*Tnfrsf1b*$^{-/-}$, hereafter named

Significance

Regulatory T (Treg) cells have been highlighted for their central function in limiting the severity of autoimmune diseases such as multiple sclerosis (MS). To date, the anatomical location and timing of this Treg cell–mediated suppression are unknown. In this report, in a mouse model of MS, we demonstrate that Treg cells inhibit the pathogenic process directly in the central nervous system during established disease, rather than in the presymptomatic phase. This protective function requires the surface expression of TNF receptor 2 by Treg cells, as its genetic ablation or antibody-mediated blockade worsens disease symptoms. Our data reveal a unique function of Treg cells in autoimmunity and highlight TNFR2 as a promising therapeutic target.

Author contributions: Y.G.-B. and B.L.S. designed research; E.R., C.P., M.K., M.H., S.G., A.C., S.K., D.S., G.H.M., N.C., Y.L., C.A., B.L., and Y.G.-B. performed research; H.W. and B.L.S. contributed new reagents/analytic tools; E.R., C.P., M.K., M.H., S.G., S.K., G.L., C.A., B.L., G.M., Y.G.-B., and B.L.S. analyzed data; and E.R., C.P., Y.G.-B., and B.L.S. wrote the paper.

The authors declare no competing interest.

This article is a PNAS Direct Submission.

[1]E.R. and C.P. contributed equally to this work.

[2]Y.G.-B. and B.L.S. contributed equally to this work.

[3]To whom correspondence may be addressed. Email: yenkel.grinberg-bleyer@inserm.fr or benoit.salomon@inserm.fr.

This article contains supporting information online at https://www.pnas.org/lookup/suppl/doi:10.1073/pnas.2014043118/-/DCSupplemental.

Published March 25, 2021.

"KO"). As previously observed (16–18), KO mice exhibited normal $CD4^+$ T cell numbers but had reduced Treg cell numbers in the spleen at steady state (*SI Appendix*, Fig. S2). These mice developed more severe EAE than wild-type (WT) controls, which was associated with reduced Treg cell accumulation in the inflamed CNS (*SI Appendix*, Fig. S3 *A* and *B*). We then generated bone marrow chimeric mice to assess the role of TNFR2 expression by hematopoietic and nonhematopoietic cells. Ablation of TNFR2 in the immune system, but not in the nonhematopoietic compartment, led to exacerbated EAE and reduced Treg cell numbers in the CNS (*SI Appendix*, Fig. S3 *C–F*). This role of TNFR2 in Treg cell expansion was a cell-autonomous mechanism, as revealed by their reduced numbers in the competitive environment of mixed bone marrow chimeras (*SI Appendix*, Fig. S3*G*).

TNFR2 Signaling in Treg Cells Mediates Disease Suppression during Overt CNS Inflammation. To further delineate the cell-autonomous role of TNFR2 in Treg cell biology, we generated mice with conditional ablation of TNFR2 in Treg cells by crossing mice expressing the CRE-recombinase in Treg cells ($Foxp3^{Cre}$) with mice carrying floxed *Tnfrsf1b* alleles ($Tnfrsf1b^{fl}$). It was critical to compare these $Foxp3^{Cre}Tnfrsf1b^{fl}$ (hereafter named conditional knockout or "cKO") mice with their proper controls, the $Foxp3^{Cre}$ mice, because of putative toxic effect of Cre expression, as recently reported (19, 20). As expected, Treg cells of cKO mice had complete ablation of TNFR2 expression (*SI Appendix*, Fig. S4*A*). However, a partial decreased TNFR2 expression was also observed on Tconv cells, which was likely due to leakiness of Cre expression in non-Treg cells in $Foxp3^{Cre}$ mice, previously reported in other mouse models (21, 22). cKO mice had no sign of spontaneous autoimmunity and displayed normal body weight (*SI Appendix*, Fig. S4*B*). Treg cell proportion, numbers, and expression of Foxp3, CD25, and CTLA-4 in lymphoid tissues were unaltered (*SI Appendix*, Fig. S4 *C* and *D*). Also, the in vitro suppressive capacity of Treg cells was not or slightly reduced by TNFR2 ablation (*SI Appendix*, Fig. S4 *E* and *F*). Therefore, TNFR2 is mainly dispensable for Treg cell homeostasis at steady state.

Next, we explored the cell-autonomous function of TNFR2 in Treg cells during CNS inflammation. Strikingly, compared with controls, cKO mice developed a very severe EAE leading to death in almost half of the mice by day 15 (Fig. 1*A*). This was not associated with increased total leukocyte infiltration in the CNS or dLN (*SI Appendix*, Fig. S5*A*). Treg cell proportions were only transiently reduced at day 10 in the CNS of cKO mice (Fig. 1*B* and *SI Appendix*, Fig. S5*B*), and the overall level of Foxp3, Ki67, CD25, or Helios was unaltered (*SI Appendix*, Fig. S5*D*). Also, TNFR2-deficient Treg cells did not acquire the capacity to produce pathogenic cytokines, such as IFNγ, IL-17A, or GM-CSF after phorbol 12-myristate 13-acetate (PMA) ionomycin stimulation in the CNS (*SI Appendix*, Fig. S5 *E* and *F*). However, further examination showed that these Treg cells in the CNS of cKO mice exhibited lower expression of CTLA-4, Blimp-1, and ICOS (Fig. 1 *C* and *D* and *SI Appendix*, Fig. S5*C*), which are markers of effector Treg cells (1, 23, 24). Interestingly, these quantitative and phenotypic Treg cell alterations in the CNS were not observed in the spleen or dLN. To further investigate whether $TNFR2^+$ Treg cell–mediated suppression of EAE occurs during the priming or effector phase, we used an inducible Cre system allowing TNFR2 ablation in Treg cells upon tamoxifen treatment. We thus generated $Foxp3^{Cre\text{-}ERT2}Tnfrsf1b^{fl}$ (hereafter named induced conditional KO or "icKO") mice. Importantly, in most of these mice, tamoxifen administration induced TNFR2 ablation in Treg cells as efficiently as in cKO mice but not at all in Tconv cells (*SI Appendix*, Fig. S6*A*). This icKO model is thus of great interest since TNFR2 ablation is Treg cell–specific contrary to cKO mice. To assess whether EAE control by TNFR2-expressing Treg cells is taking place in the CNS after disease onset, we administered tamoxifen from day 7 to 14 after disease induction. Remarkably, EAE severity was dramatically increased in icKO when compared with $Foxp3^{Cre\text{-}ERT2}$ control animals, similarly to what we observed with cKO mice (Fig. 2*A*). At day 14, total leukocyte numbers, Treg cell proportions and numbers as well as their Foxp3 expression remained unaltered in CNS and dLN of icKO mice (Fig. 2*B* and *SI Appendix*, Fig. S6 *B–D*). Treg cell proportion was also normal at day 10 (*SI Appendix*, Fig. S6*E*). The proportion of activated $CD44^{high}CD62L^{low}$ Treg cells was unchanged in dLN and CNS between icKO and control mice (*SI Appendix*, Fig. S7*A*). Also, Treg cells specific for the myelin oligodendrocyte glycoprotein 35–55 peptide $(MOG)_{35–55}$, the immunizing antigen in EAE, were present in similar proportions in icKO and control mice in both dLN and CNS (*SI Appendix*, Fig. S7*B*). However, TNFR2-deficient Treg cells expressed lower levels of CTLA-4 and Blimp-1 in the CNS (Fig. 2 *C* and *D*), as observed in cKO mice. Once again, this altered Treg cell phenotype was not observed in the dLN, which is compatible with a disease control by $TNFR2^+$ Treg cells in the inflamed CNS rather than in the dLN. Moreover, this suggests that TNFR2 was not involved in the initial activation steps but rather in the acquisition of an optimal immunosuppressive state by Treg cells after day 7.

To further address the mechanism of EAE exacerbation, we performed RNA-sequencing on Treg cells from the CNS and dLN of icKO and control mice at day 14. In the inflamed CNS, a number of important genes exhibited altered expression in mutant Treg cells (Fig. 2 *E* and *F*). For instance, the expression of several genes associated with the highly suppressive effector Treg cell subset, such as *Myb*, *Ccr8*, and *Cd177* (25), was downregulated in TNFR2-deficient Treg cells. Surprisingly, mRNA expression of *Ctla4* and *Prdm1* (Blimp-1) remained unchanged, suggesting that TNFR2 ablation in Treg cells may lead to post-transcriptional modifications. Conversely, genes usually associated with Tconv cell effector function, such as granzymes and perforin, and even *Cd8a* and *Cd8b* genes, displayed augmented expression in mutant Treg cells. Gene set enrichment analyses (GSEA) revealed an enrichment of the $CD8^+$ Tconv cell signature in mutant Treg cells (*SI Appendix*, Fig. S8*A*). This was not due to cell contamination of the samples as mutant Treg cells expressed normal amounts of *Cd4* and *Zbtb7b* (ThPOK), as well as *Tbx21*, *Runx1*, or *Runx3*, compared with WT Treg cells (*SI Appendix*, Fig. S8*B*). To confirm these data, some of the differentially expressed genes were analyzed at protein level in the CNS. *CD8a*, *Thy1* (coding for CD90), and *Eomes* that had higher level of mRNA in TNFR2-deficient Treg cells (*SI Appendix*, Fig. S8*C*), also displayed increased protein expression (*SI Appendix*, Fig. S8*D*). Importantly, the increased CD8α expression was due to a slight shift of the whole Treg cell population and not to the presence of few cells expressing high level of CD8, definitively ruling out the hypothesis of the presence of $CD8^+$ Tconv cell contaminants. Interestingly, expression of the long noncoding RNA *Flicr*, which was described to negatively regulate *Foxp3* expression and Treg cell function (26), was increased in the absence of TNFR2. GSEA further confirmed that TNFR2-deficient Treg cells were less activated and did not acquire the full identity of Treg cells from the inflamed CNS, when compared with control Treg cells (Fig. 2*G*). Importantly, the differential expression of these genes in TNFR2-deficient Treg cells was not seen in dLNs, in which only subtle decrease in genes involved in homing such as *Ccr1*, *Itga5*, or *Itgam* was observed (*SI Appendix*, Fig. S9 *A* and *B*). Altogether, these results show that the loss of TNFR2 expression by Treg cells induces alteration of their activation and identity during EAE, specifically in the CNS and not in the dLN.

TNFR2 Expression by Treg Cells Limits the Activation and Pathogenic Function of Tconv Cells in the CNS. We then characterized the pathogenic profile of CD4 Tconv cells. Quite surprisingly, they acquired a similar $CD44^{high}CD62L^{low}$ activated phenotype in icKO and control mice and expressed equivalent amounts of the

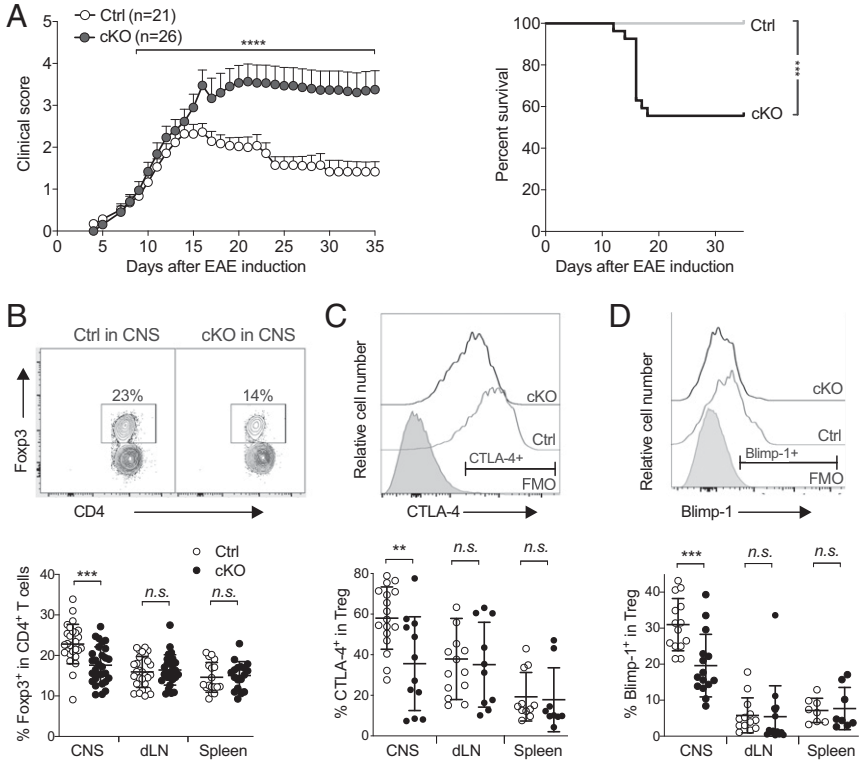

Fig. 1. Exacerbated EAE and impaired CNS Treg cell homeostasis in mice with constitutive ablation of TNFR2 in Treg cells. EAE was induced in *Foxp3*-^{Cre}*Tnfrsf1b*^{fl} (cKO) and *Foxp3*^{Cre} control (Ctrl) mice. (*A*) EAE clinical score and disease survival. (*B–D*) FACS phenotyping at D10. Proportion of Treg cells (*B*) and of CTLA-4 (*C*) and Blimp-1 (*D*) expression among Treg cells is shown as mean ± SD from four independent experiments with each symbol representing a mouse. *Upper* panels show representative dot plots and histograms of CNS Treg cells. Two-tailed, unpaired Mann–Whitney *U* (*A*, for EAE scores, and *B–D*), and log-rank (Mantel–Cox, *A*, for survival curves) were used; $^{**}P < 0.01$, $^{***}P < 0.001$, $^{****}P < 0.0001$; *n.s.*, nonsignificant.

pathogenic GM-CSF after strong polyclonal PMA ionomycin restimulation in dLN and CNS (*SI Appendix*, Fig. S10 *A* and *B*). Also, $MOG_{35–55}$–specific Tconv cells were present in similar proportions in both types of mice in dLN and CNS (*SI Appendix*, Fig. S10*C*). More informative data were obtained when we performed transcriptomic analyses at day 14. In line with the aggravated EAE symptoms and the impairment of the Treg cell gene expression profile in icKO mice, transcriptomic analyses of $CD4^+$ Tconv cell counterparts in the CNS showed major alterations. The expression of 185 and 229 genes was respectively down- and up-regulated in Tconv cells isolated from mutant animals, compared with controls (Fig. 3*A*). Tconv cells from icKO mice displayed a highly activated phenotype. Notably, mRNA of cytokines and chemokines (*Csf2*, *Il22*, *Ifng*, *Tnf*, *Il2*, *Lta*, *Ccl3*, *Ccl4*) and cytokine receptors and chemokine receptors as well as other activation markers (*Il2ra*, *Il12r*, *Ifngr*, *Ccr2*, *Ccr5*, *Icos*, *Fasl*, *Ctla4*, *Gzmb*) were significantly increased in these cells (Fig. 3*B* and *SI Appendix*, Fig. S9*C*). They also expressed increased levels of genes of signaling pathways (such as MAPK and NF-κB), interferon signature (*Ifit*, *Isg*), and transcription factors (*Prdm1*, *Bhlhe40*, *Rora*, *Egr1*, *Fosl2*, *Junb*), known to be up-regulated in activated T cells. Accordingly, the expression of genes characterizing resting T cells were down-regulated in Tconv cells from the CNS of icKO mice, such as *Sell* (CD62L), *Ly6c1*, *Ccr7*, *Klf2*, *Bach2*, *Tcf7*, or *Lef1* (Fig. 3*B*). Among genes up-regulated in Tconv cells of icKO mice, network analysis of putative protein–protein interactions connected two nodes, one regrouping genes coding for activation markers with the other one belonging to an interferon signature. Interestingly, these two nodes were connected by the *Tnf* and *Ifng* genes (*SI Appendix*, Fig. S9*D*). The metabolic profile icKO Tconv cells further supports their activated status with increased expression of most genes of the glycolytic pathway as well as of *Slc2a1* (Glut1), the main glucose transporter in T cells, and *Hif1a*, a master positive regulator of glycolysis (Fig. 3*C* and *SI Appendix*, Fig. S9*C*). GSEA further confirmed that these icKO Tconv cells had an activated status (Fig. 3*D*). Not only these Tconv cells have an activated status, but also their transcriptome suggests a Th1/Th17 pathogenic profile with increased expression of *Csf2* (GM-CSF), *Il22*, *Ifng*, *Ifngr*, or *Il12r*. We confirmed some of these results at the protein level by measuring cytokines produced by CNS-infiltrating cells isolated at day 14 by enzyme-linked immunosorbent assay (ELISA). GM-CSF, which is the major pathogenic cytokine produced by Tconv cells in EAE (27), was significantly increased in icKO mice compared with control mice after both anti-CD3 and immunizing myelin antigen stimulation (Fig. 3*E*). IL-17A and IFN-γ production were slightly increased in icKO Tconv cells as well but not significantly. All these modified expression patterns (gene expression and cytokine expression) were not observed—or at a much lower extent—in the dLN (*SI Appendix*, Fig. S9 *E–G*). Altogether, these data strongly suggest that TNFR2 expression by Treg cells is involved in the local suppression of activated and pathogenic Tconv cells in the CNS after disease onset, but not in their initial priming in lymphoid tissues.

TNF/TNR2 Signaling in Treg Cells Enables Local Suppression of EAE in the Inflamed CNS. We then conducted experiments to further confirm the CNS-restricted role of TNFR2-expressing Treg cells. In the course of active EAE, the disease is initiated in dLN and spleen. Then, from day 5, pathogenic Tconv cells migrate to the CNS where they are reactivated, leading to their progressive accumulation and increased inflammation, perpetuating locally the disease process (28). We first analyzed the phenotype of T cells during priming in lymphoid tissues to evaluate their capacity to acquire pathogenic features. We assessed expression of

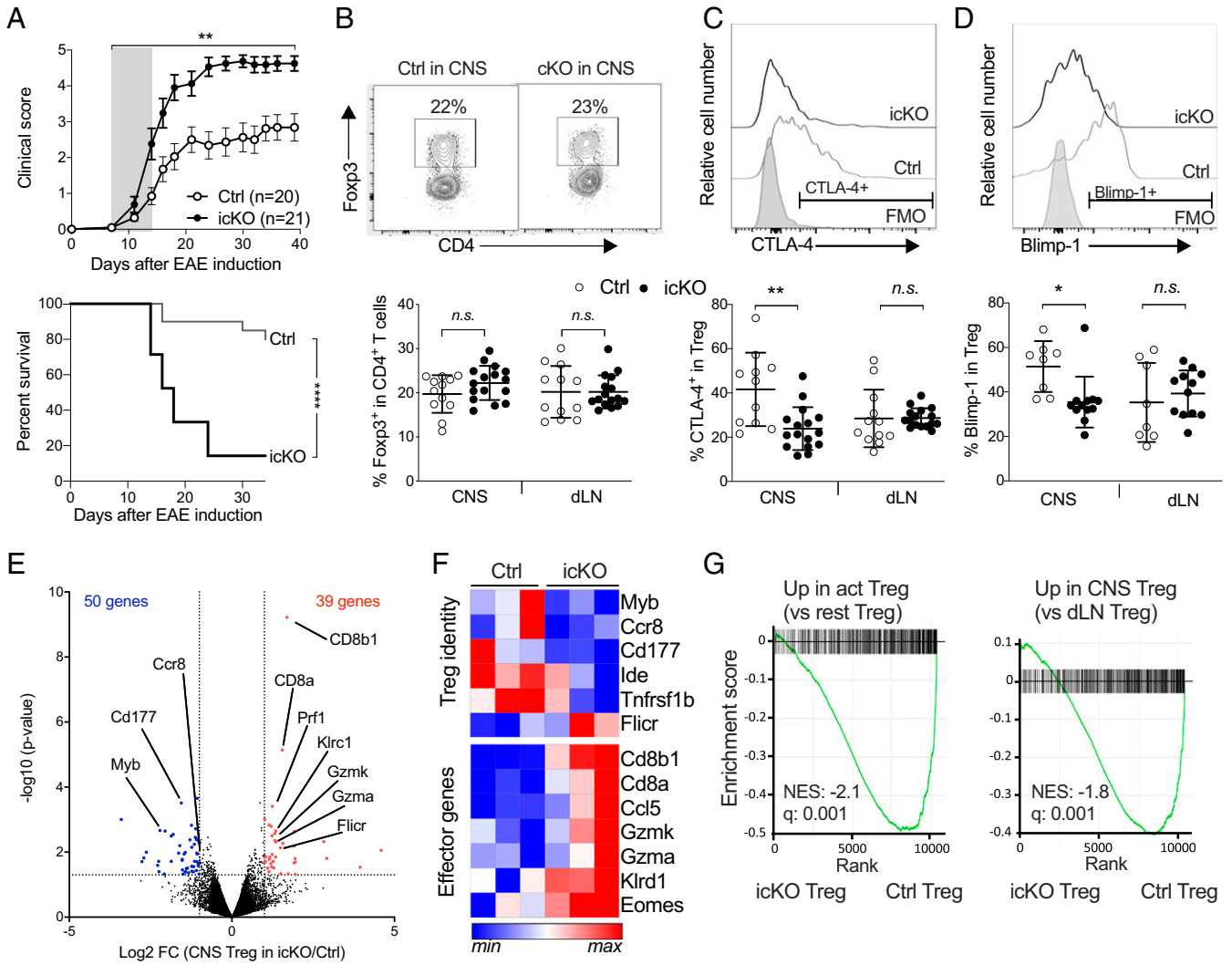

Fig. 2. Ablation of TNFR2 in Treg cells after disease onset induced exacerbated EAE and impaired Treg cell activation in the CNS. *Foxp3*$^{Cre\text{-}ERT2}$*Tnfrsf1b*^{fl} (icKO) and *Foxp3*$^{Cre\text{-}ERT2}$ control (Ctrl) mice were immunized to induce EAE at day 0 and treated with tamoxifen from day 7 to 14. (*A*) EAE clinical score and disease survival. (*B–D*) FACS phenotyping at D14. Proportion of Treg cells (*B*) and of CTLA-4 (*C*) and Blimp-1 (*D*) expression among Treg cells is shown as mean ± SD from four independent experiments with each symbol representing a mouse. *Upper* panels show representative dot plots and histograms of CNS Treg cells. (*E–G*) Gene expression analysis of CNS-infiltrating Treg cells at day 14. (*E*) Volcano plot depicting differentially expressed genes. (*F*) Heatmap showing expression of selected genes. (*G*) GSEA plots of icKO Treg cells compared with genes up-regulated in 36-h culture in vitro activated vs. resting Treg cells (*Left*) or with genes up-regulated in CNS vs. dLN Treg cells (*Right*). Two-tailed, unpaired Mann–Whitney *U* (*A*, for EAE scores, and *B–D*) and log-rank (Mantel–Cox, *A*, for survival curve) were used; **P* < 0.05, ***P* < 0.01, *****P* < 0.0001; *n.s.*, nonsignificant.

CD11a (LFA-1 α chain), CXCR3, CCR6, and CD49d (VLA-4 α chain) because of their involvement in T cell migration from lymphoid tissues to inflamed CNS during EAE (29, 30). Ten days after EAE induction, these molecules were expressed at the same levels in control and cKO mice, suggesting unaltered migration capacity into the CNS (*SI Appendix*, Fig. S11). To more directly quantify priming of MOG-reactive T cells, we transferred T cell receptor-transgenic Tconv cells specific for this antigen in cKO and control mice. Then, mice were immunized with $MOG_{35–55}$ peptide, and we measured the activation of donor cells in dLN and spleen 3 and 7 d later. The level of T cell proliferation and expansion was high and comparable in the two groups of mice (Fig. 4*A* and *SI Appendix*, Fig. S12 *A* and *B*). Donor MOG-specific T cells expressed similar levels of CD11a and CD49d and of the IFNγ, IL-17A, and GM-CSF pathogenic cytokines after PMA–ionomycin stimulation in cKO mice compared with controls (*SI Appendix*, Fig. S12 *C* and *D*). Together with the unchanged proportions of MOG-reactive T cells we detected in icKO animals (*SI Appendix*, Fig. S10*C*), these data suggest a normal priming of MOG-specific Tconv cells in lymphoid tissues in both cKO and icKO mice. To further assess the pathogenicity of polyclonal MOG-specific T cells primed in dLN, we measured their capacity to induce EAE after adoptive transfer in naive mice. Remarkably, cells primed in cKO and control mice, and restimulated ex vivo, induced similar passive EAE (Fig. 4*B*). Thus, all these data concur to show that exacerbation of EAE in cKO mice was not due to enhanced initial priming of MOG-specific T cells in spleen and dLN. Then, to further confirm that TNFR2-expressing Treg cells selectively controlled EAE severity within the inflamed CNS, we transferred WT pathogenic T cells to cKO or control naive mice. In this setting, injected cells rapidly migrated into the CNS to damage the neural tissue during passive EAE, without being primed in the dLN. Strikingly, EAE was much more severe in cKO than control recipients (Fig. 4*C*). We obtained similar findings when we transferred pathogenic T cells in WT recipients that were treated with an anti-TNF blocking mAb

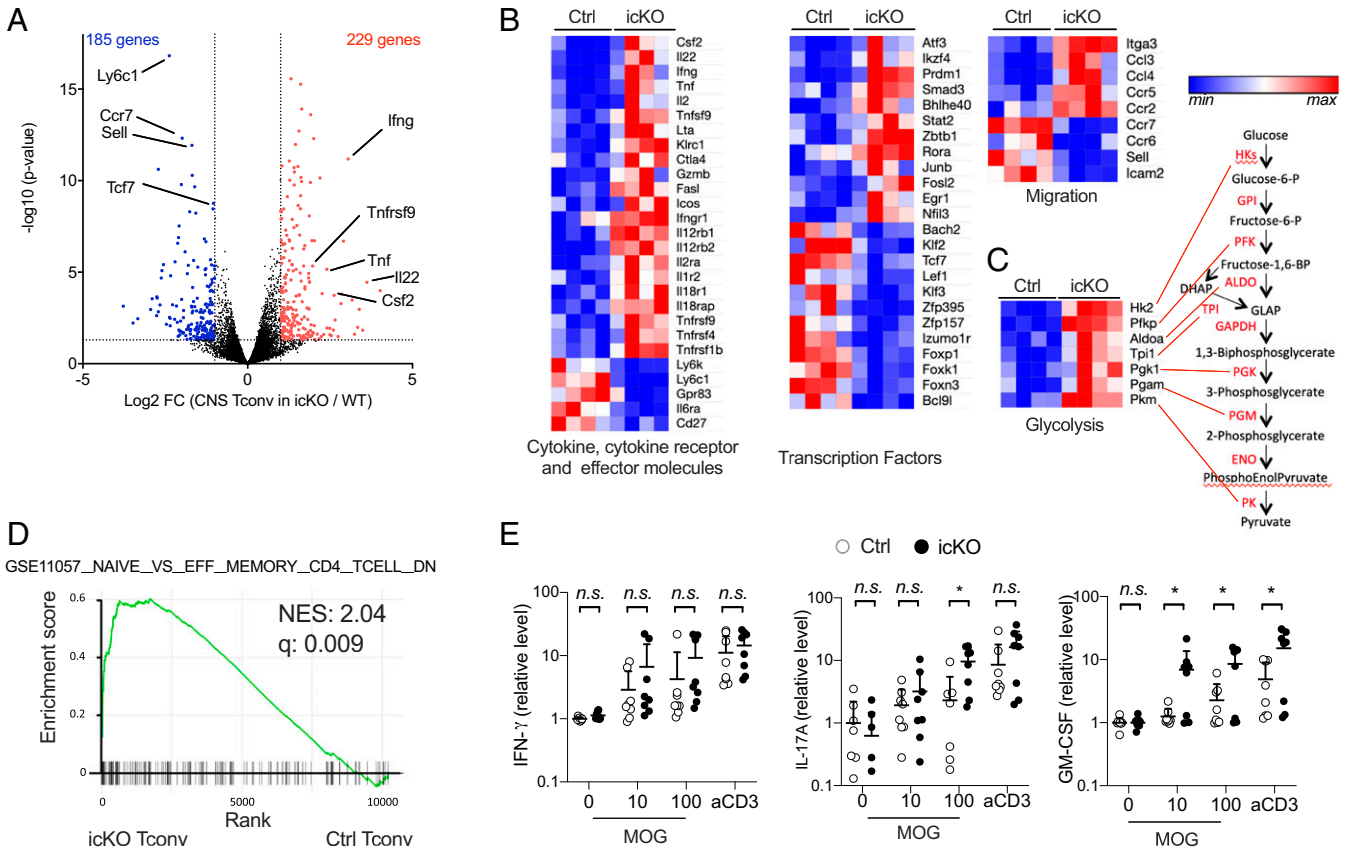

Fig. 3. TNFR2 expression by Treg cells limits the activation and pathogenic function of Tconv cells in the CNS. EAE was induced in *Foxp3*$^{Cre\text{-}ERT2}$*Tnfrsf1b*^{fl} (icKO) and *Foxp3*$^{Cre\text{-}ERT2}$ control (Ctrl) mice that were treated with tamoxifen as in Fig. 2, and cells were analyzed at day 14. (*A–D*) Transcriptomic analyses on purified CD4^{+}Foxp3^{-} Tconv cells, isolated from the CNS. (*A*) Volcano plot depicting differentially expressed genes. (*B*) Heatmaps showing expression of selected genes (FDR < 0.05) coding for cytokine, cytokine receptor, and T cell effector molecules (*Left*), transcription factors (*Middle*), and molecules involved in T cell migration (*Right*). (*C*) Heatmaps showing expression of selected genes (FDR < 0.05) coding enzymes of the glycolytic pathway (*Left*) and their position in the pathway (*Right*). (*D*) GSEA plots of icKO Tconv cells compared with genes up-regulated in effector memory versus naive CD4 T cells from the indicated GSE pathway. (*E*) Cytokines produced by CNS-infiltrating leukocytes restimulated ex vivo by the immunizing MOG antigen (10 or 100 μg/mL) or an anti-CD3 mAb were measured by ELISA in the supernatants. Graphs show the fold change concentration over control unstimulated cells (No Stim). Pool of two independent experiments with each symbol representing an individual mouse. Two-way unpaired ANOVA test with Sidak correction for multiple comparisons. *$P < 0.05$; *n.s.*, nonsignificant.

(Fig. 4*D*). Taken together, these results confirm our earlier findings that TNFR2 signaling in Treg cells is critical to control EAE within the inflamed CNS, rather than limiting the priming of pathogenic T cells in lymphoid tissues.

Systemic Modulation of the TNF/TNFR2 Axis Affects EAE Severity. The protective facet of TNF in CNS autoimmunity relied originally on observations made in patients. Indeed, anti-TNF therapies are formally contraindicated in MS patients because of disease exacerbation (31, 32). The mechanism of this long-term conundrum, well known to clinicians, remains essentially unexplained. To investigate whether our earlier findings could bring a mechanistic insight to this adverse effect of anti-TNF treatments, we assessed the effect of this therapy on EAE severity and Treg cell phenotype in EAE. WT mice were treated with a blocking anti-TNF mAb from day 10—a time when they developed the first clinical signs—until day 18. As observed in MS patients, these mice exhibited an aggravated form of EAE compared with isotype-control treated mice (Fig. 5*A*). Similar findings were obtained when using the clinically approved soluble TNFR2-Fc fusion receptor (Etanercept) to block TNF (Fig. 5*B*). Interestingly, TNF-blockade at earlier time points (from day 0) did not significantly modify the course of the disease (Fig. 5*C*), highlighting once more the protective role of TNF during established disease and not during Tconv cell priming. We next analyzed the Treg cell compartment in the inflamed CNS of these mice. In anti-TNF–treated mice, Treg cell proportion was significantly reduced in the CNS compared with control animals, whereas it was unchanged in dLN. These observations are similar to the ones we previously made in TNFR2 conditional KO mice and further support the CNS-restricted role of TNF on Treg cells (Fig. 5*D*). This protective effect of TNF was most likely due to TNFR2 triggering since blocking this receptor with a specific mAb worsened EAE (Fig. 5*E*), similarly to anti-TNF mAb treatment or TNFR2 ablation in Treg cells. Finally, from a therapeutic perspective, we investigated whether stimulating TNFR2 signaling in the course of the disease could improve disease outcome. Remarkably, the use of a TNFR2-specific agonist from day 4 to 18 significantly reduced EAE severity (Fig. 5*F*). This therapeutic effect was lost in icKO animals, suggesting that this agonist functions by stimulating TNFR2-expressing Treg cells (*SI Appendix*, Fig. S13). Collectively, these data are in line with our previous findings, highlighting the protective role of TNF in CNS during EAE and providing a mechanistic explanation for the deleterious events following anti-TNF administration in patients with MS.

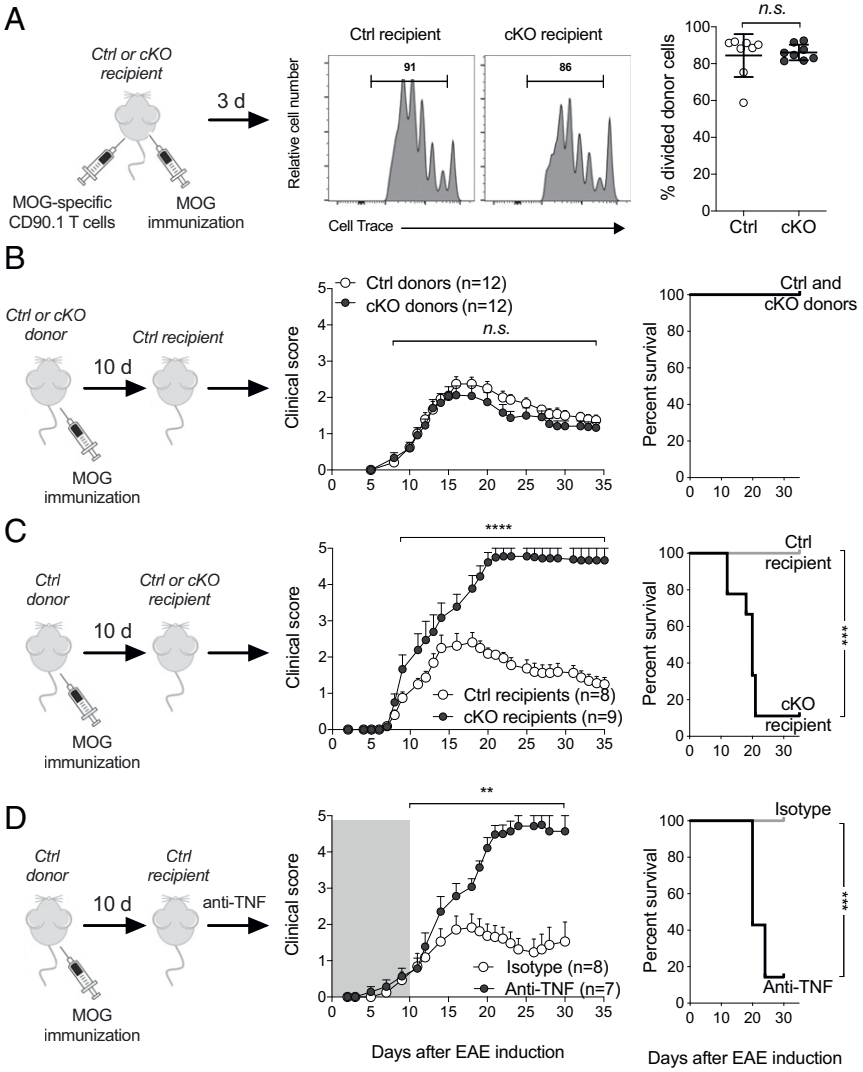

Fig. 4. TNF/TNFR2 signaling in Treg cells enables local suppression of EAE in the inflamed CNS. (*A*) Representative division profile (*Left*) and cumulative percentages of divided cells (*Right*) of MOG-specific CD90.1$^+$ Tconv cells 3 d after transfer in *Foxp3*^{Cre}*Tnfrsf1b*^{fl} and *Foxp3*^{Cre} mice immunized to induce EAE. (*B*) Clinical score and disease survival of passive EAE induced in WT recipients transferred with pathogenic cells obtained from dLN of *Foxp3*^{Cre}*Tnfrsf1b*^{fl} (cKO) or *Foxp3*^{Cre} control (Ctrl) mice immunized 10 d earlier to induce EAE. (*C*) Clinical score and disease survival of passive EAE induced in cKO or control recipients transferred with pathogenic cells obtained from dLN of WT mice immunized 10 d earlier to induce EAE. (*D*) Clinical score and disease survival of passive EAE induced in WT recipients transferred with pathogenic cells obtained from dLN of WT mice immunized 10 d earlier to induce EAE. Recipients were treated with an anti-TNF or isotype control (Ctrl) mAb from day 0 to 8 after cell transfer. Data are from four (*A*) and two (*B–D*) independent experiments. In *A*, mean (±SD) from four experiments is shown; each dot represents a mouse. Unpaired *t* test was used. In *B–D*, mean (+SEM) from two experiments is shown. Two-tailed, unpaired Mann–Whitney *U* (for EAE scores and FACS analyses) and log-rank tests (Mantel–Cox, for survival curves) were used; $^{**}P < 0.01$, $^{***}P < 0.001$, $^{****}P < 0.0001$; *n.s.*, nonsignificant.

Discussion

The protective properties of Treg cells in autoimmune diseases are clearly established. However, when and where do endogenous Treg cells control these diseases remain unknown. Some published works provided indirect evidence that Treg cells may suppress an autoimmune disease in the target organ. Indeed, late accumulation of Treg cells was observed in the inflamed CNS during EAE (6, 33, 34). Systemic Treg cell deletion precipitated established autoimmune diseases but at the expense of massive and multifocal inflammation, precluding a proper evaluation of physiological function of Treg cells (6, 35). Administration of Treg cells specific for the target tissue had a therapeutic efficacy in organ-specific autoimmune diseases, suggesting a capacity to suppress pathogenic cells locally (36, 37). However, these studies did not address the role of endogenous Treg cells during the natural course of the disease. Here, we found that TNFR2 ablation in Treg cells after EAE induction had no systemic impact but led to increased CNS inflammation and disease severity. This suggested that Treg cells suppressed EAE at peak of disease in the inflamed CNS and not during T cell priming in the dLN. This hypothesis was further supported by the following cumulative proofs. 1) Treg cell phenotype, and their proportion in some models, were altered in the CNS but not in the dLN in cKO mice, icKO mice, or WT mice treated with anti-TNF drugs. 2) Increased expression of activation molecules and pathogenic GM-CSF by Tconv cells could be observed in the CNS of icKO mice but not in dLN. The increased production of GM-CSF in icKO mice was no longer observed after PMA–ionomycin stimulation, probably because this strong and nonphysiological activation could outweigh the difference observed with more physiological

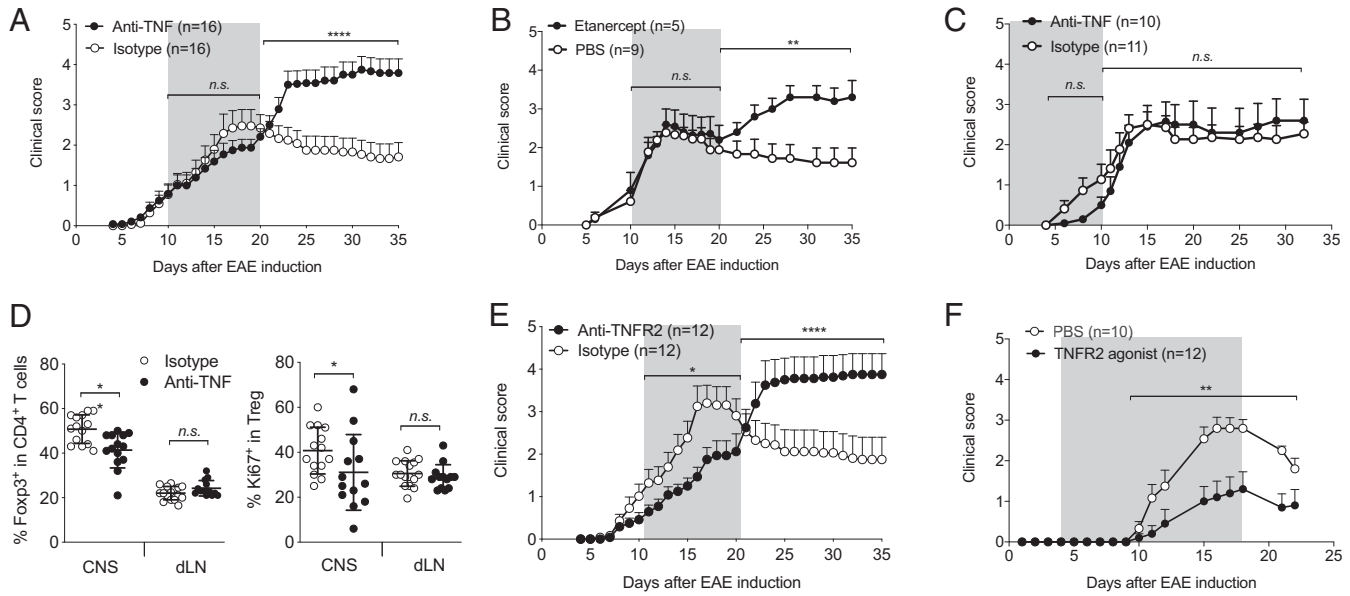

Fig. 5. Systemic modulation of the TNF/TNFR2 axis affects EAE severity. (*A–C*) EAE clinical score in C57BL/6 mice immunized to induce EAE (day 0) and treated with anti-TNF, or isotype control mAbs or Etanercept for the indicated periods of time (gray boxes). Mean (+SEM) from two (*B*) or three (*A* and *C*) independent experiments. (*D*) Proportions of Treg cells and of dividing Treg cells in the CNS and dLN of mice treated with anti-TNF mAb as in *A*, and analyzed at days 29 to 45. Mean (±SD) from five experiments; each dot represents a mouse. (*E*) EAE clinical score in mice treated with a blocking anti-TNFR2 or isotype control mAbs from day 10 to 18. Mean from two independent experiments. (*F*) EAE clinical score in mice treated from day 4 to 18 with a TNFR2 agonist. Mean (+SEM) from two independent experiments. Two-tailed unpaired Mann–Whitney *U* test was used. $*P < 0.05$, $**P < 0.01$, $****P < 0.0001$; *n.s.*, nonsignificant.

T cell receptor stimulation. 3) Activation and expansion in lymphoid tissues and migration into the CNS of polyclonal and MOG-specific T cells appeared normal in cKO and icKO mice, compared with control mice. 4) Blocking TNF in WT mice from day 10, but not from day 0, after disease induction led to EAE exacerbation, suggesting that the early autoimmune process that was primed in dLN was not altered by the absence of TNFR2 in Treg cells. In the same line, disease exacerbation following TNFR2 ablation in Treg cells was obtained when this deletion obtained by tamoxifen administration was performed 7 d after disease induction. 5) Cell transfer experiments showed that the activation of myelin-specific T cells in spleen and dLN, as well as their capacity to induce passive EAE, were largely similar in cKO and control mice. However, it remains possible that the ex vivo restimulation protocol, which is required to induce disease, may have skewed the potential differences between Tconv cells from the two strains. 6) Finally, pathogenic T cells from WT mice that were reactivated in the CNS after their injection induced a more severe disease in cKO than in control recipients. Thus, the control of EAE by TNFR2-expressing Treg cells is regulated in the inflamed CNS and not in the dLN. Together, our work strongly supports the concept that endogenous Treg cells suppress an autoimmune disease in the target tissue.

Our findings also provide some insight into the mechanism of EAE control by Treg cells in the CNS. Indeed, TNFR2 expression by Treg cells appears to control their function rather than their numbers. We did find a decreased proportion of Treg cells in the CNS at day 10 in cKO mice, but this was no more observed earlier (day 7) or later (day 15) in these mice or in the icKO animals. More importantly, TNFR2-deficient Treg cells have lower mRNA expression of several Treg cell–signature genes and increased expression of genes normally expressed by Tconv cells. Also, TNFR2-deficient Treg cells expressed a lower level of *Myb* that was shown to be essential for differentiation of effector Treg cells (25). The lack of TNFR2 expression in Treg cells seems to have an additional impact on protein expression, as observed for CTLA-4 and Blimp-1, whose protein levels were decreased in CNS of icKO mice. This may alter Treg cell suppressive activity, as CTLA-4 is one of the major mechanisms of Treg cell–mediated suppression and Blimp-1 is critical to promote IL-10 production (1, 23, 24). Also, Blimp-1 is expressed by the fraction of highly suppressive effector Treg cells and is up-regulated in CNS Treg cells during EAE. Moreover, its ablation in Treg cells led to exacerbated EAE, reduced Treg cell identity, and increased expression of inflammatory cytokines, such as IL-17 (2, 3). Consequently, TNFR2-deficient Treg cells would be deficient in suppressing Tconv cells in the CNS, leading to massive Tconv cell activation, as observed at the level of activation markers, cytokines and chemokines, signaling molecules, transcription factors, and glucose metabolism. These highly activated Tconv cells produced an increased level of pathogenic cytokines such as GM-CSF, precipitating EAE. In conclusion, our data demonstrate that TNFR2 expression by Treg cells is essential to limit EAE severity by promoting their transient expansion and by increasing their suppressive function in the CNS, thereby limiting pathogenic Tconv cell activation. Thus, we reveal here a nonredundant function of TNF in the control of EAE in the inflamed CNS. Recent findings emphasized the critical role of IL-33 in the accumulation of Treg cells residing in the intestine or adipose tissues (38–40). Thus, depending on the tissue and type of inflammation, Treg cells may rely on different environmental cues (IL-33 and TNF) for their homeostasis and function.

Besides this nonredundant function of TNFR2 in Treg cells, our data also bring a mechanistic explanation to the deleterious effect of TNF blockade in patients with MS. A series of preclinical studies in mice conducted in the nineties concluded that blocking TNF was beneficial in EAE (reviewed in ref. 41). These findings led to initiate two clinical trials in MS patients that had to be rapidly stopped because of disease aggravation (31, 32). Here, we revisited this question using reagents that selectively block TNF, whereas older studies used drugs blocking both TNF and lymphotoxin-α, which is an issue since the latter cytokine is pathogenic in EAE (42). We found that blocking TNF at

Table 1. mAbs and fluorescent reagents used in this study

mAb or reagent	Clone	Vendor	Reference	Dilution
BV510 anti-mouse CD4	RM4-5	BD Biosciences	563106	1/500
BUV496 anti-mouse CD4	GK1.5	BD Biosciences	564667	1/400
Alexa Fluor 700 anti-mouse CD8a	53-6.7	BD Biosciences	557959	1/400
BUV805 anti-mouse CD8a	53-6.7	BD Biosciences	564920	1/400
PerCP-C5.5 anti-mouse CD11a	2D7	BD Biosciences	562809	1/100
Biotin anti-mouse CD25	7D4	BD Biosciences	553070	1/300
PE-Cy7 anti-mouse CD44	IM7	Invitrogen/eBioscience	25-0441-82	1/400
BUV395 anti-mouse CD45	30-F11	BD Biosciences	564279	1/400
PE-CF594 anti-mouse CD45	30-F11	BD Biosciences	562420	1/1000
PE anti-mouse CD45.1	A20	BD Biosciences	561872	1/100
Biotin anti-mouse CD45.1	A20	Miltenyi	130101902	1/10
PE anti-mouse CD49d	R1-2	BD Biosciences	553157	1/100
AF700 anti-mouse CD62L	MEL-14	BD Biosciences	560517	1/100
APC anti-mouse CD90.1	OX-7	BD Biosciences	561409	1/400
PE-Cy7 anti-mouse ICOS	7E.17G9	Invitrogen/eBioscience	25-9942-82	1/400
PE anti-mouse CTLA-4 (CD152)	UC104F10-11	BD Biosciences	553720	1/200
Alexa Fluor 647 anti-mouse Blimp-1	5E7	BD Biosciences	563643	1/100
PE-Cy7 anti-mouse Eomes	Dan11mag	Invitrogen/eBioscience	25-4875-80	1/100
BV421 anti-mouse TNFR2 (CD120b)	TR75-89	BD Biosciences	564088	1/200
FITC anti-mouse GITR	DTA-1	BD Biosciences	558139	1/200
PE anti-mouse Vβ11	RR3-15	BD Biosciences	553198	1/200
BV421 anti-mouse CCR6	140706	BD Biosciences	564736	1/20
APC anti-mouse CXCR3	CXCR3-173	BD Biosciences	562266	1/100
APC anti-human/mouse Foxp3	FJK-16s	Invitrogen/eBioscience	17-5773-82	1/200
FITC anti-human/mouse Foxp3	FJK-16s	Invitrogen/eBioscience	11-5773-82	1/200
PE-e610 anti-huma/mouse Foxp3	FJK-16s	Invitrogen/eBioscience	61-5773-82	1/100
eF450 anti mouse/human Ki67	SOLA15	Invitrogen/eBioscience	48-5698-82	1/400
AF647 anti-mouse IFNg	XMG1.2	BD Biosciences	557735	1/100
APC-Cy7 anti-mouse IL-17A	TC11-18H10	BD Biosciences	560821	1/100
PE anti-mouse GM-CSF	MP1-22E9	BD Biosciences	554406	1/100
BV421 streptavidin		BD Biosciences	563259	1/400
PE-Cy7 streptavidin		Invitrogen/eBioscience	25-4317-82	1/200
e450 cell trace		Life Technologies		1/2,000
e506 fixable viability dye		Invitrogen/eBioscience	65-0866-14	1/1,000

disease's peak induced EAE exacerbation, as in MS patients who were also treated during advanced disease progression. Interestingly, when TNF was blocked at earlier times, EAE was not exacerbated, and even slightly delayed. Thus, at disease initiation, TNF might be pathogenic by activating antigen-presenting cells via TNFR1, whereas it would regulate the disease afterward, by activating Treg cells via TNFR2 in the inflamed CNS. In this line, blocking TNFR1 at disease induction attenuated EAE (43), whereas we showed that blocking TNFR2 at day 10 induced disease exacerbation, similarly to late TNFR2 ablation in Treg cells. Furthermore, we demonstrated that stimulation of TNFR2 signaling reduced EAE severity.

In conclusion, our data reveal that the TNF/TNFR2 axis is critical to reach an optimal Treg cell function specifically in the CNS during EAE, thereby preventing excessive inflammation and controlling disease severity. Moreover, our results bring insights in the mechanism of autoimmune disease control by Treg cells and provide an explanation for the failure of anti-TNF therapy in MS patients, paving the way to the development of more specific treatments aiming at the selective blockade of TNFR1 and/or selective stimulation of TNFR2.

Methods

Mice. C57BL/6J (WT) mice were purchased from Janvier Labs (France). *Tnfrsf1b*^{tm1Mwm}/J (*Tnfrs1b*$^{-/-}$), *Foxp3*$^{tm9(EGFP/cre/ERT2)Ayr}$/J (*Foxp3*$^{Cre\text{-}ERT2}$), and C57BL/6 Tg (Tcra2D2,Tcrb2D2)1Kuch/J (2D2) T cell receptor transgenic mice, specific for myelin oligodendrocyte glycoprotein, were purchased from The Jackson Laboratory. *Cd3*^{etm1Mal} (*Cd3*$^{-/-}$), CD45.1, and CD90.1 mice were provided by the Cryopreservation Distribution Typing and Animal Archiving Department (Orléans, France). B6.129(Cg)-*Foxp3*$^{tm4(YFP/icre)Ayr}$/J (*Foxp3*^{Cre}) mice were a gift from Prof. Alexander Rudensky, Memorial Sloan Kettering Cancer Center, New York, NY. C57BL/6-*Tnfrsf1b*$^{<tm1c(EUCOMM)Wtsi>}$/Ics (*Tnfrsf1b*^{fl}) mice were obtained from the EMMA Consortium. All mice were on a C57BL/6J background or have been backcrossed at least 10 times to C57BL/6J mice. Mice were housed under specific pathogen-free conditions and were studied at 7 to 14 wk of age or 2 mo after bone marrow transplant.

TNF- and TNFR2-Targeting Biological. Anti-TNF (XT3-11) and anti-TNFR2 (TR75-54.7) mAbs were purchased from BioXCell and were injected at a dose of 500 μg by intraperitoneal route every other day for 8 or 14 d. Etanercept (TNFR2-Fc) was provided by Wyeth and was administered at a dose of 1 mg by intraperitoneal route every other day for 8 d. Purification and functional characterization of the TNFR2-specific agonist STAR2 have been described elsewhere (10).

Bone Marrow Transplantation. Bone marrow cells were isolated from tibia and femur of donor mice. Recipient mice were lethally irradiated (10.5 Gy) and transplanted intravenously with 10×10^6 bone marrow cells. EAE was induced at least 8 wk after transplantation.

EAE Induction. For active EAE, mice were injected subcutaneously in the flanks with 100 μg of MOG_{35-55} peptide (Polypeptide) emulsified in 100 μL of complete Freund adjuvant (Sigma-Aldrich) supplemented with 50 μg of heat-killed *Mycobacterium tuberculosis* H37Ra (BD Biosciences). Animals were additionally injected intravenously with 200 ng of *Bordetella pertussis* toxin (Enzo) at the time of immunization and 2 d later. For the passive EAE model, we first induced active EAE in donor mice as described above to generate pathogenic

cells. Ten days postimmunization, cells from spleen and dLN were cultured in complete RPMI (Gibco) medium with 10% fetal calf serum at 5×10^6 cells/mL with 20 μg/mL $MOG_{35–55}$ peptide, 10 μg/mL anti-IFNγ (XMG1.2, BioXCell), and 5 ng/mL IL-23 (R&D Systems). After 3 d, dead cells were removed with a Ficoll gradient, and 2×10^6 cells were injected intravenously to recipient mice to induce passive EAE. The clinical evaluation was performed on a daily basis by a six-point scale ranging from 0, no clinical sign; 1, limp tail; 2, limp tail, impaired righting reflex, and paresis of one limb; 3, hindlimb paralysis; 4, hindlimb and forelimb paralysis; to 5, moribund/death. A score of 5 was permanently attributed to dead animals.

Preparation of Cell Suspensions. For isolation of CNS-infiltrating leukocytes, mice were anesthetized with a xylazine/ketamine solution and perfused with cold PBS. Spinal cords were removed by intrathecal hydrostatic pressure. Brain and spinal cords were cut into small pieces and digested in RPMI 1640 (Gibco) supplemented with 1 mg/mL collagenase type IV (Sigma), 100 μg/mL DNase I (Sigma), and 1 μg/mL TLCK for 30 min at 37 °C followed by mechanical desegregation. Single-cell suspensions were washed once and resuspended in Percoll 40%. For fluorescence-activated cell sorting (FACS) analysis, cells were laid on a Percoll 80% solution, centrifuged for 20 min at 2,000 rpm at room, and mononuclear cells were collected from the interface of the 40:80% Percoll gradient and were washed two times in a PBS–3% fetal calf serum buffer. For FACS cell sorting, cells were centrifuged for 10 min at 400 × *g* and mononuclear cells were collected from the pellet of the monolayer Percoll gradient. Cells from thymus, spleen, and LN were obtained after mechanical dilacerations.

Antibodies and Flow Cytometry Analysis. The mAbs and fluorescent reagents used in this study are listed Table 1. Intracellular staining was performed using the Foxp3/Transcription Factor Staining Buffer Set kit and protocol from eBioscience. Identification of MOG-specific T cells was performed using the I-A(b) mouse MOG 38–49 GWYRSPFSRVVH APC-labeled tetramer, obtained from the NIH Tetramer Facility, according to their protocol. Intracellular cytokine staining (*SI Appendix*, Figs. S5, S10, and S12) was assessed after 4 h of PMA (25 ng/mL)–ionomycin (1 mg/mL) stimulation in RPMI 1640 containing 10% FCS and Golgi plug (BD Biosciences).

Cells were acquired on a BD LSRII cytometer and analyzed using the FlowJo software.

Treg and Tconv Cell Purification. For suppression assay, colitis and transcriptomic analyses, cell suspensions from the spleen, LN, or the CNS were stained with e780 viability dye, BV510 anti-CD4 (RM4-5), and PE-CF594 anti-CD45 (30F11) mAbs. Purified Tconv cells ($CD4^+YFP^-$ or $CD4^+GFP^-$) and Treg cells ($CD4^+YFP^+$ or $CD4^+GFP^+$) were obtained using a BD FACSAria II. For transcriptomic analyses, cells were sorted twice with the cytometer leading to over 99.8% purity.

Cell Culture. Culture medium was composed of RPMI 1640 (Gibco) supplemented with 10% fetal calf serum. For suppression assay, purified Tconv cells (2.5×10^4 cells/well), labeled with CellTrace Violet (Proliferation Kit; Life Technologies), and purified Treg cells were stimulated by splenocytes from $Cd3^{-/-}$ mice (7.5×10^4 cells/well) and soluble anti-CD3 mAb (0.05 μg/mL 2C11; BioXCell) in 96-well plate at different Treg/Tconv cell ratios. At day 3, CellTrace dilution was assessed by flow cytometry. To assess TNFR2 expression, whole splenocytes (3×10^6 cells/well) were stimulated by soluble anti-CD3 (5 μg/mL 2C11; BioXCell) in 96-well plate. For ELISA studies (Fig. 3 and *SI Appendix*, Fig. S9), cells from 3.5×10^6 LN cells in 2 mL in 24-well plates or 1×10^5 CNS cells in 200 μL in 96-round bottom well plates were stimulated with 10 or 100 μg/mL MOG or with 5 μg/mL anti-CD3 mAb (2C11) for 24 h (CNS cells) or 72 h (LN cells) before performing ELISA on the supernatant using kits from Invitrogen.

Adoptive Transfer of 2D2 T Cells. LN and spleen cells from 2D2 CD90.1 or 2D2 CD45.1 mice were stained incubated with anti-CD19 (6D5), anti-CD11b (M1/70), anti-CD11c (N418), anti-CD8 (53-6.7), and anti-CD25 (7D4) biotin-labeled mAbs, and then were coated with anti-biotin microbeads (Miltenyi Biotec). After magnetic sorting, cells of the $CD4^+$ enriched negative fraction were labeled with CellTrace Violet Proliferation Kit and were intravenously injected in naive mice (10^6 cells/mouse). The following day, mice were immunized with $MOG_{35–55}$ peptide as for EAE induction. Donor cells, identified by their $CD4^+CD90.1^+V\beta11^+$ (T cell receptor transgene) or $CD45.1^+CD3^+$ phenotypes, were analyzed by flow cytometry in dLNs and spleen 3 or 7 d later.

RNA-Sequencing and Bioinformatics Analyses. RNA was extracted from highly purified Treg and Tconv cells using the NucleoSpin RNA XS kit from Macherey-Nagel, quantified using a ND-1000 NanoDrop spectrophotometer (NanoDrop Technologies), and purity/integrity was assessed using disposable RNA chips (Agilent High Sensitivity RNA ScreenTape) and an Agilent 2200 Tapestation (Agilent Technologies). mRNA library preparation was performed following manufacturer's recommendations (SMART-Seq v4 Ultra Low Input RNA Kit; TAKARA). Final-17 samples pooled library prep was sequenced on NextSeq 500 Illumina with HighOutPut cartridge (2×400 million of 75 base reads), corresponding to 2 times 23×10^6 reads per sample after demultiplexing. Poor quality sequences have been trimmed or removed with Trimmomatic software to retain only good quality paired reads. Star v2.5.3a (44) has been used to align reads on reference genome mm10 using standard options. Quantification of gene and isoform abundances has been done with rsem 1.2.28 (45) prior to normalization on library size with DESEq2 bioconductor package. Finally, differential analysis has been conducted with edgeR bioconductor package. Multiple hypothesis adjusted *P* values were calculated with the Benjamini–Hochberg procedure to control false-discovery rate (FDR). For Treg cells, data were obtained from a biological triplicate. For Tconv cells, data were obtained from two independent experiments with biological quadruplicate, after exclusion of two outliers. GSEA has been done with fGSEA bioconductor R package (v1.12.0) on preranked list. Genes in our dataset (GSE165821) were ranked according to the signed fold-change multiplied by the −log10 *P* value of the differential analysis. Gene sets were extracted from GSE165821 (Fig. 2 *G*, *Right*), GSE146135 (Fig. 2 *G*, *Left*), and GSE11057 (Fig. 3*D*).

Statistics. Statistical analyses were performed using GraphPad Prism software, version 8.3.1. For EAE scores and two-group comparisons, statistical significance was determined using the two-tailed unpaired nonparametric Mann–Whitney *U* test, excluding D0 to D5 as all scores were 0. For survival curves, log-rank (Mantel–Cox) test was used. For ELISAs, two-way unpaired ANOVA test with Sidak correction for multiple comparisons was used. $*P < 0.05$, $**P < 0.01$, $***P < 0.001$, and $****P < 0.0001$.

Study Approval. All experimental protocols were approved by Comité d'Éthique en Expérimentation Animal Charles Darwin No. 5 under number 02811.03 and are in compliance with European Union guidelines.

Data Availability. The RNA-seq data reported in this paper have been deposited in the Gene Expression Omnibus (GEO) database, https://www.ncbi.nlm.nih.gov/geo (accession no. GSE165821). All other study data are included in the article and/or *SI Appendix*.

ACKNOWLEDGMENTS. This work was supported by the Agence Nationale de la Recherche Grants (ANR-15-CE15-0015-03, ANR-17-CE15-0030-01), Fondation pour la Recherche Médicale (équipe FRM), Fondation Bettencourt Schueller (to B.L.S.), Association de la Recherche sur la Sclérose en Plaques (to B.L.S. and Y.G.-B.), the ATIP-Avenir Young Investigator Program (to Y.G.-B.), Institut Français de Recherche et d'Enseignement Supérieur à l'International (to M.K.), and Deutsche Forschungsgemeinschaft Grants (324392634–TRR 221, WA 1025/31-1) (to H.W.). We are grateful to Prof. Alexander Rudensky for providing us with the Foxp3Cre mice, to Prof. Jeffrey Bluestone and Matthew Krummel for critical reading of the manuscript, to Dr. Lennart Mars for providing us with the 2D2 mice, and to Doriane Foret, Flora Issert, Olivier Bregerie, and Maria Mihoc for their expert care of the mouse colony. We thank the NIH Tetramer Facility for providing us with the MOG tetramer. We are grateful for the great expertise of Yannick Marie, Delphine Bouteiller, Beata Gyorgy, and Justine Guegan from the bioinformatic platform of Institut du Cerveau et de la Moelle Epinière (Paris).

1. E. Cretney *et al.*, The transcription factors Blimp-1 and IRF4 jointly control the differentiation and function of effector regulatory T cells. *Nat. Immunol.* **12**, 304–311 (2011).
2. G. Garg *et al.*, Blimp1 prevents methylation of Foxp3 and loss of regulatory T cell identity at sites of inflammation. *Cell Rep.* **26**, 1854–1868.e5 (2019).
3. C. Ogawa *et al.*, Blimp-1 functions as a molecular switch to prevent inflammatory activity in $Foxp3^+ROR\gamma t^+$ regulatory T cells. *Cell Rep.* **25**, 19–28.e5 (2018).
4. S. Z. Josefowicz, L. F. Lu, A. Y. Rudensky, Regulatory T cells: Mechanisms of differentiation and function. *Annu. Rev. Immunol.* **30**, 531–564 (2012).
5. J. B. Wing, A. Tanaka, S. Sakaguchi, Human $FOXP3^+$ regulatory T cell heterogeneity and function in autoimmunity and cancer. *Immunity* **50**, 302–316 (2019).
6. M. J. McGeachy, L. A. Stephens, S. M. Anderton, Natural recovery and protection from autoimmune encephalomyelitis: Contribution of $CD4^+CD25^+$ regulatory cells within the central nervous system. *J. Immunol.* **175**, 3025–3032 (2005).

7. A. P. Kohm, P. A. Carpentier, H. A. Anger, S. D. Miller, Cutting edge: $CD4^+CD25^+$ regulatory T cells suppress antigen-specific autoreactive immune responses and central nervous system inflammation during active experimental autoimmune encephalomyelitis. *J. Immunol.* **169**, 4712–4716 (2002).
8. S. Hori, M. Haury, A. Coutinho, J. Demengeot, Specificity requirements for selection and effector functions of $CD25^+4^+$ regulatory T cells in anti-myelin basic protein T cell receptor transgenic mice. *Proc. Natl. Acad. Sci. U.S.A.* **99**, 8213–8218 (2002).
9. X. Chen, M. Bäumel, D. N. Männel, O. M. Howard, J. J. Oppenheim, Interaction of TNF with TNF receptor type 2 promotes expansion and function of mouse $CD4^+CD25^+$ T regulatory cells. *J. Immunol.* **179**, 154–161 (2007).
10. M. Chopra *et al*., Exogenous TNFR2 activation protects from acute GvHD via host T reg cell expansion. *J. Exp. Med.* **213**, 1881–1900 (2016).
11. Y. Grinberg-Bleyer *et al*., Pathogenic T cells have a paradoxical protective effect in murine autoimmune diabetes by boosting Tregs. *J. Clin. Invest.* **120**, 4558–4568 (2010).
12. M. Leclerc *et al*., Control of GVHD by regulatory T cells depends on TNF produced by T cells and TNFR2 expressed by regulatory T cells. *Blood* **128**, 1651–1659 (2016).
13. B. Zaragoza *et al*., Suppressive activity of human regulatory T cells is maintained in the presence of TNF. *Nat. Med.* **22**, 16–17 (2016).
14. S. Yang *et al*., Differential roles of TNFα-TNFR1 and TNFα-TNFR2 in the differentiation and function of $CD4^+Foxp3^+$ induced Treg cells in vitro and in vivo periphery in autoimmune diseases. *Cell Death Dis.* **10**, 27 (2019).
15. K. N. Atretkhany *et al*., Intrinsic TNFR2 signaling in T regulatory cells provides protection in CNS autoimmunity. *Proc. Natl. Acad. Sci. U.S.A.* **115**, 13051–13056 (2018).
16. L. Probert *et al*., TNFR1 signalling is critical for the development of demyelination and the limitation of T-cell responses during immune-mediated CNS disease. *Brain* **123**, 2005–2019 (2000).
17. G. C. Suvannavejh *et al*., Divergent roles for p55 and p75 tumor necrosis factor receptors in the pathogenesis of $MOG_{35–55}$-induced experimental autoimmune encephalomyelitis. *Cell. Immunol.* **205**, 24–33 (2000).
18. N. Tsakiri, D. Papadopoulos, M. C. Denis, D. D. Mitsikostas, G. Kollias, TNFR2 on non-haematopoietic cells is required for $Foxp3^+$ Treg-cell function and disease suppression in EAE. *Eur. J. Immunol.* **42**, 403–412 (2012).
19. B. Becher, A. Waisman, L. F. Lu, Conditional gene-targeting in mice: Problems and solutions. *Immunity* **48**, 835–836 (2018).
20. M. Kurachi, S. F. Ngiow, J. Kurachi, Z. Chen, E. J. Wherry, Hidden caveat of inducible cre recombinase. *Immunity* **51**, 591–592 (2019).
21. P. D. Bittner-Eddy, L. A. Fischer, M. Costalonga, Cre-loxP reporter mouse reveals stochastic activity of the *Foxp3* promoter. *Front. Immunol.* **10**, 2228 (2019).
22. D. Franckaert *et al*., Promiscuous Foxp3-cre activity reveals a differential requirement for CD28 in $Foxp3^+$ and $Foxp3^-$ T cells. *Immunol. Cell Biol.* **93**, 417–423 (2015).
23. K. Wing *et al*., CTLA-4 control over $Foxp3^+$ regulatory T cell function. *Science* **322**, 271–275 (2008).
24. C. Neumann *et al*., Role of Blimp-1 in programing Th effector cells into IL-10 producers. *J. Exp. Med.* **211**, 1807–1819 (2014).
25. S. Dias *et al*., Effector regulatory T cell differentiation and immune homeostasis depend on the transcription factor Myb. *Immunity* **46**, 78–91 (2017).
26. D. Zemmour, A. Pratama, S. M. Loughhead, D. Mathis, C. Benoist, *Flicr*, a long noncoding RNA, modulates Foxp3 expression and autoimmunity. *Proc. Natl. Acad. Sci. U.S.A.* **114**, E3472–E3480 (2017).
27. L. Codarri *et al*., RORγt drives production of the cytokine GM-CSF in helper T cells, which is essential for the effector phase of autoimmune neuroinflammation. *Nat. Immunol.* **12**, 560–567 (2011).
28. S. L. Bailey, B. Schreiner, E. J. McMahon, S. D. Miller, CNS myeloid DCs presenting endogenous myelin peptides "preferentially" polarize $CD4^+$ T_H-17 cells in relapsing EAE. *Nat. Immunol.* **8**, 172–180 (2007).
29. F. Sallusto *et al*., T-cell trafficking in the central nervous system. *Immunol. Rev.* **248**, 216–227 (2012).
30. R. Sporici, T. B. Issekutz, CXCR3 blockade inhibits T-cell migration into the CNS during EAE and prevents development of adoptively transferred, but not actively induced, disease. *Eur. J. Immunol.* **40**, 2751–2761 (2010).
31. The Lenercept Multiple Sclerosis Study Group and The University of British Columbia MS/MRI Analysis Group, TNF neutralization in MS: Results of a randomized, placebo-controlled multicenter study. *Neurology* **53**, 457–465 (1999).
32. B. W. van Oosten *et al*., Increased MRI activity and immune activation in two multiple sclerosis patients treated with the monoclonal anti-tumor necrosis factor antibody cA2. *Neurology* **47**, 1531–1534 (1996).
33. T. Korn *et al*., Myelin-specific regulatory T cells accumulate in the CNS but fail to control autoimmune inflammation. *Nat. Med.* **13**, 423–431 (2007).
34. R. A. O'Connor, K. H. Malpass, S. M. Anderton, The inflamed central nervous system drives the activation and rapid proliferation of $Foxp3^+$ regulatory T cells. *J. Immunol.* **179**, 958–966 (2007).
35. M. Feuerer, Y. Shen, D. R. Littman, C. Benoist, D. Mathis, How punctual ablation of regulatory T cells unleashes an autoimmune lesion within the pancreatic islets. *Immunity* **31**, 654–664 (2009).
36. L. A. Stephens, K. H. Malpass, S. M. Anderton, Curing CNS autoimmune disease with myelin-reactive $Foxp3^+$ Treg. *Eur. J. Immunol.* **39**, 1108–1117 (2009).
37. Q. Tang *et al*., In vitro-expanded antigen-specific regulatory T cells suppress autoimmune diabetes. *J. Exp. Med.* **199**, 1455–1465 (2004).
38. C. Schiering *et al*., The alarmin IL-33 promotes regulatory T-cell function in the intestine. *Nature* **513**, 564–568 (2014).
39. D. Kolodin *et al*., Antigen- and cytokine-driven accumulation of regulatory T cells in visceral adipose tissue of lean mice. *Cell Metab.* **21**, 543–557 (2015).
40. A. Vasanthakumar *et al*., The transcriptional regulators IRF4, BATF and IL-33 orchestrate development and maintenance of adipose tissue-resident regulatory T cells. *Nat. Immunol.* **16**, 276–285 (2015).
41. C. A. Dendrou, J. I. Bell, L. Fugger, A clinical conundrum: The detrimental effect of TNF antagonists in multiple sclerosis. *Pharmacogenomics* **14**, 1397–1404 (2013).
42. W. E. Suen, C. M. Bergman, P. Hjelmström, N. H. Ruddle, A critical role for lymphotoxin in experimental allergic encephalomyelitis. *J. Exp. Med.* **186**, 1233–1240 (1997).
43. S. K. Williams *et al*., Antibody-mediated inhibition of TNFR1 attenuates disease in a mouse model of multiple sclerosis. *PLoS One* **9**, e90117 (2014).
44. A. Dobin *et al*., STAR: Ultrafast universal RNA-seq aligner. *Bioinformatics* **29**, 15–21 (2013).
45. B. Li, C. N. Dewey, RSEM: Accurate transcript quantification from RNA-seq data with or without a reference genome. *BMC Bioinformatics* **12**, 323 (2011).